J|A|C|S
ARTICLES
Published on Web 09/20/2002

Reconstructing NMR Spectra of "Invisible" Excited Protein States Using HSQC and HMQC Experiments

Nikolai R. Skrynnikov,*,†,§ Frederick W. Dahlquist,‡ and Lewis E. Kay†

Contribution from the Protein Engineering Network Center of Excellence, Departments of Medical Genetics, Biochemistry and Chemistry, University of Toronto, Toronto, Ontario, Canada M5S 1A8, Department of Chemistry, Purdue University, West Lafayette, Indiana 47907, and Institute of Molecular Biology and Department of Chemistry, University of Oregon, Eugene, Oregon 97403

Received May 20, 2002. Revised Manuscript Received July 23, 2002

Abstract: Carr−Purcell−Meiboom−Gill (CPMG) relaxation measurements employing trains of 180° pulses with variable pulse spacing provide valuable information about systems undergoing millisecond-time-scale chemical exchange. Fits of the CPMG relaxation dispersion profiles yield rates of interconversion, relative populations, and absolute values of chemical shift differences between the exchanging states, $|\Delta\omega|$. It is shown that the sign of $\Delta\omega$ that is lacking from CPMG dispersion experiments can be obtained from a comparison of chemical shifts in the indirect dimensions in either a pair of HSQC (heteronuclear single quantum coherence) spectra recorded at different magnetic fields or HSQC and HMQC (heteronuclear multiple quantum coherence) spectra obtained at a single field. The methodology is illustrated with an application to a cavity mutant of T4 lysozyme in which a leucine at position 99 has been replaced by an alanine, giving rise to exchange between ground state and excited state conformations with a rate on the order of 1450 s^{-1} at 25 °C.

Introduction

Protein dynamics is critical for function. For example, enzyme catalysis, ligand binding to macromolecules, and molecular recognition all involve motion.[1−5] Often these dynamical processes include traversing from highly populated ground states to very much less populated, although biologically important, excited states. In these cases a complete description of the states involved is necessary in order to understand the relationship between structure, dynamics, and function. Many powerful biophysical methods are available to study the abundant state(s). In contrast, however, the low populations of the excited states render their analysis much more difficult.

Solution state NMR relaxation dispersion studies of molecules undergoing conformational exchange on a microsecond-to-millisecond time scale provide a powerful approach for the characterization of these excited states. In dispersion experiments the effective decay of the magnetization is measured as a function of an applied B_1 radio frequency field and, if the exchange time scale is favorable, the data are fitted to obtain the exchange lifetimes of the states, their relative populations, and the chemical shift differences between the conformations involved.[6] Processes occurring on a submillisecond time scale are best studied using off-resonance rotating frame spin relaxation methods.[7,8] Recently, Trott and Palmer have extended the formalism describing the evolution of exchanging systems in the presence of an off-resonance field to include the case where exchange is not in the fast limit (i.e., the exchange rate is not required to exceed the chemical shift difference, $\Delta\omega$, between states).[9] In principle, in favorable cases it is now possible to obtain not only the magnitude of the chemical shift difference but also the sign of the difference. This sign information is critical if the shift differences are to be interpreted properly in terms of structural changes between the exchanging conformers.

In cases where the exchange is on a millisecond time scale, the Carr−Purcell−Meiboom−Gill (CPMG)-based scheme in which relaxation rates are recorded as a function of the spacing between refocusing pulses is particularly useful.[10,11] Recently, new methods have been developed allowing measurement of exchange parameters at multiple backbone and side-chain sites in a protein.[12−14] In these experiments exchange processes are

* Address correspondence to this author. E-mail: nikolai@purdue.edu.
† University of Toronto.
‡ University of Oregon.
§ Purdue University.

(1) Eisenmesser, E. Z.; Bosco, D. A.; Akke, M.; Kern, D. *Science* **2002**, *295*, 1520−1523.
(2) Wang, J.; Ortiz-Maldonado, M.; Entsch, B.; Massey, V.; Ballou, D.; Gatti, D. L. *Proc. Natl. Acad. Sci. U.S.A.* **2002**, *99*, 608−613.
(3) Horst, R.; Damberger, F.; Luginbuhl, P.; Guntert, P.; Peng, G.; Nikonova, L.; Leal, W. S.; Wüthrich, K. *Proc. Natl. Acad. Sci. U.S.A.* **2001**, *98*, 14374−14379.
(4) Zhong, D. P.; Douhal, A.; Zewail, A. H. *Proc. Natl. Acad. Sci. U.S.A.* **2000**, *97*, 14056−14061.
(5) Leulliot, N.; Varani, G. *Biochemistry* **2001**, *40*, 7947−7956.
(6) Palmer, A. G.; Kroenke, C. D.; Loria, J. P. *Methods Enzymol.* **2001**, *339*, 204−238.
(7) Desvaux, H.; Birlikakis, N.; Wary, C.; Bertahult, P. *Mol. Phys.* **1995**, *86*, 1059−1073.
(8) Akke, M.; Palmer, A. G. *J. Am. Chem. Soc.* **1996**, *118*, 911−912.
(9) Trott, O.; Palmer, A. G. *J. Magn. Reson.* **2002**, *154*, 157−160.
(10) Carr, H. Y.; Purcell, E. M. *Phys. Rev.* **1954**, *94*, 630−638.
(11) Meiboom, S.; Gill, D. *Rev. Sci. Instrum.* **1958**, *29*, 688−691.
(12) Loria, J. P.; Rance, M.; Palmer, A. G. *J. Am. Chem. Soc.* **1998**, *121*, 2331−2332.

10.1021/ja0207089 CCC: $22.00

separated from the effects of spin−spin relaxation and scalar coupling evolution, thereby extending the range of time scales that can be probed,[12] and data acquisition times are reduced by use of a constant-time relaxation scheme.[13,15] Unfortunately, only the magnitude of chemical shift differences, $|\Delta\omega|$, can be obtained using these experiments because they essentially concentrate on exchange-induced line *broadening* which carries no information about the sign of $\Delta\omega$. In contrast, exchange-induced *shifts* readily provide information about the signs of interest, as demonstrated in this work.

We present here a number of simple and sensitive experiments for measuring the sign of $\Delta\omega$ in systems with millisecond-time-scale exchange which are best suited for analysis using CPMG-based dispersion measurements. Specifically, we show that a comparison of peak positions in the heteronuclear (indirect) dimensions of HSQC and HMQC spectra recorded at a single spectrometer field or in HSQC spectra recorded at two different fields allows, in most cases, unambiguous determination of the sign. The methodology is illustrated through an application to a cavity mutant of T4 lysozyme in which a leucine residue at position 99 is replaced by an alanine.[16] This protein, termed L99A, is able to bind substituted benzenes at rates on the order of 1000 s^{-1} (k_1[benzene] + k_{-1}), at room temperature.[17] Previous studies have shown that L99A exchanges between a (ground) ligand-inaccessible state and a (excited) ligand-accessible state and have led to a detailed characterization of the exchange process as a function of temperature.[13,14,18−20] Here we report the sign of $\Delta\omega$ for the backbone ^{15}N spins in the excited conformer of L99A (3% population at 25 °C), a first step in characterizing the structural differences between the ground and excited states.

Theory

Consider a two-site exchange process, $A \underset{k_b}{\overset{k_a}{\rightleftharpoons}} B$, where the populations of the species are strongly skewed, $p_a \gg p_b$, $k_a \ll k_b$, so that only the resonances from the dominant (ground state) species, A, can be observed in spectra. Focusing on a spin coherence, V, and assuming that this coherence is not coupled to any others, we can write the following equation for the evolution of V:

$$\frac{d}{dt}\begin{bmatrix}V_a(t)\\V_b(t)\end{bmatrix} = \begin{bmatrix}-i\omega_a - k_a - R_a & k_b\\ k_a & -i\omega_b - k_b - R_b\end{bmatrix}\begin{bmatrix}V_a(t)\\V_b(t)\end{bmatrix} \quad (1)$$

where $V_a(t)$ and $V_b(t)$ are the amounts of coherence V in each of the two exchanging states (assumed proportional to the populations p_a, p_b), ω_a and ω_b are the Zeeman frequencies in rad s^{-1}, k_a and k_b are forward and backward exchange rates, $k_a + k_b = k_{ex}$, and R_a and R_b are spin relaxation rates. The solution to eq 1 can be formulated as

$$\begin{bmatrix}V_a(t)\\V_b(t)\end{bmatrix} = \exp(-i\omega_a t - R_a t) \times \exp\left(\begin{bmatrix}-k_a & k_b\\ k_a & -i\Delta\omega - k_b - \Delta R\end{bmatrix} t\right)\begin{bmatrix}V_a(0)\\V_b(0)\end{bmatrix} \quad (2)$$

where the evolution due to chemical exchange is contained in the second exponential in eq 2; $\Delta\omega = \omega_b - \omega_a$ and $\Delta R = R_b - R_a$ are the differences in resonance frequencies and relaxation rates between coherences $V_a(t)$ and $V_b(t)$, respectively. Note that V is an arbitrary coherence in this treatment. For example, the evolution of double-quantum coherence from an isolated two-spin system of an amide group, N_+H_+, is described by eq 2 with $\Delta\omega = \Delta\omega_N + \Delta\omega_H = (\omega_N^b - \omega_N^a) + (\omega_H^b - \omega_H^a)$.

Solving the characteristic equation for the matrix in eq 2 and retaining the leading term with respect to the small parameter $k_a/(k_b + \Delta R + i\Delta\omega)$, we obtain expressions for exchange broadening of the observable spectral line (site a) and the exchange-induced shift for this line:

$$R^{ex} = k_a\frac{\rho(1+\rho)+\xi^2}{(1+\rho)^2+\xi^2} \quad (3.1)$$

$$\delta^{ex} = k_a\frac{\xi}{(1+\rho)^2+\xi^2} \quad (3.2)$$

where $\rho = \Delta R/k_b$ and $\xi = \Delta\omega/k_b$. This is in agreement with the results of Anet and Basus,[21] who calculated NMR line shapes for the case of strongly skewed exchanging populations assuming $\Delta R = 0$. In this paper we focus on the exchange-induced shifts, eq 3.2. The expression for the shift δ^{ex} has a very simple functional form, and it is clear that $\delta^{ex} \to 0$ in the limiting cases of infinitely fast, $\xi \to 0$, or infinitely slow, $\xi \to \infty$, exchange.

Although the theoretical treatment can be readily formulated in a completely general manner, we prefer to discuss the specific case involving ^{15}N spins since the experimental results in this work are derived from analysis of ^{15}N−^{1}H correlation spectra. To examine the dependence on static magnetic field strength, B_0, it is convenient to express the frequency shifts in parts per million (ppm), $\Delta\omega_N = \gamma_N B_0 \Delta\tilde{\omega}_N$, $\delta_N^{ex} = \gamma_N B_0 \tilde{\delta}_N^{ex}$, where $\Delta\omega/2\pi$ and $\delta_{ex}/2\pi$ are in hertz (Hz) and $\Delta\tilde{\omega}$ and $\tilde{\delta}^{ex}$ are in ppm,[22] with a tilde henceforth used to indicate shift values in ppm, and γ_N is the gyromagnetic ratio of nitrogen. Making this substitution in eq 3.2 gives $\tilde{\delta}_N^{ex} = k_a\tilde{\xi}_N/((1+\rho)^2 + (\gamma_N B_0\tilde{\xi}_N)^2)$, where $\tilde{\xi}_N = \Delta\tilde{\omega}_N/k_b$, and it is clear that $\tilde{\delta}_N^{ex}$ decreases with increasing magnetic field strength. From here it follows that the positions of peaks in spectra recorded at magnetic field $B_0^{(i)}$ are shifted with respect to their positions in spectra recorded at a field strength of $B_0^{(ii)}$ by

$$\tilde{\sigma}_N = \frac{k_a\tilde{\xi}_N}{(1+\rho)^2 + (\gamma_N B_0^{(i)}\tilde{\xi}_N)^2} - \frac{k_a\tilde{\xi}_N}{(1+\rho)^2 + (\gamma_N B_0^{(ii)}\tilde{\xi}_N)^2} \quad (4)$$

where $\tilde{\sigma}_N$ is in ppm. Considering, for example, the shifts in the F1(^{15}N) dimension of an HSQC correlation map, we note that at 500 MHz the peaks from exchanging residues are shifted closer (in ppm) to the invisible resonances of the minor species

(13) Mulder, F. A. A.; Skrynnikov, N. R.; Hon, B.; Dahlquist, F. W.; Kay, L. E. *J. Am. Chem. Soc.* **2001**, *123*, 967−975.
(14) Skrynnikov, N. R.; Mulder, F. A. A.; Hon, B.; Dahlquist, F. W.; Kay, L. E. *J. Am. Chem. Soc.* **2001**, *123*, 4556−4566.
(15) Tollinger, M.; Skrynnikov, N. R.; Mulder, F. A. A.; Forman-Kay, J. D.; Kay, L. E. *J. Am. Chem. Soc.* **2001**, *123*, 11341−11352.
(16) Eriksson, A. E.; Baase, W. A.; Zhang, X.-J.; Heinz, D. W.; Blaber, M.; Baldwin, E. P.; Matthews, B. W. *Science* **1992**, *255*, 178−183.
(17) Feher, V. A.; Baldwin, E. P.; Dahlquist, F. W. *Nat. Struct. Biol.* **1996**, *3*, 516−521.
(18) Mulder, F. A. A.; Hon, B.; Muhandiram, D. R.; Dahlquist, F. W.; Kay, L. E. *Biochemistry* **2000**, *39*, 12614−12622.
(19) Mulder, F. A. A.; Mittermaier, A.; Hon, B.; Dahlquist, F. W.; Kay, L. E. *Nat. Struct. Biol.* **2001**, *8*, 932−935.
(20) Mulder, F. A. A.; Hon, B.; Mittermaier, A.; Dahlquist, F. W.; Kay, L. E. *J. Am. Chem. Soc.* **2002**, *124*, 1443−1451.
(21) Anet, F. A. L.; Basus, V. J. *J. Magn. Reson.* **1978**, *32*, 339−343.
(22) Levitt, M. H. *J. Magn. Reson.* **1997**, *126*, 164−182.

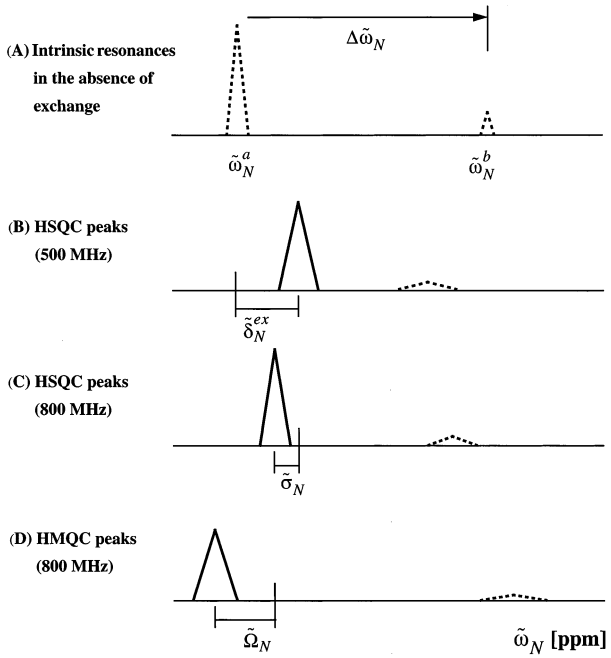

Figure 1. Schematic representation of ^{15}N resonance frequencies and shifts in a system undergoing two-site exchange. Observable peaks are drawn with solid lines; hypothetical peaks for the case of no chemical exchange (A) and peaks broadened beyond detection by chemical exchange (B−D) are drawn with dashed lines. The position of the HMQC peak can, in general, be shifted to the left or the right of the intrinsic resonance, $\tilde{\omega}_N^a$, depending on the values of ξ_H and ξ_N (in panel D the peak is drawn to the left). However, so long as eq 6 is fulfilled, the HSQC peak is positioned closer to the intrinsic resonance of the minor peak, $\tilde{\omega}_N^b$, than the HMQC peak. Although the value of the exchange-induced shift $\tilde{\delta}_{ex}$ by itself is impossible to measure because there is no suitable reference point, both $\tilde{\Omega}$ and $\tilde{\sigma}$ can be determined experimentally.

than at 800 MHz (see Figure 1). This means that, in principle, *the sign of $\Delta\omega_N$ is encoded in a pair of regular HSQC spectra recorded at different magnetic field strengths*.

As a next step, we use the example of a ^{1}H−^{15}N amide spin system to examine the difference between the frequencies recorded in single-quantum and multiple-quantum experiments. From eq 3.2 it follows immediately that in the presence of chemical exchange that can affect both proton and nitrogen spins, cross-peaks in HSQC spectra are shifted in the F1(^{15}N) dimension by an amount Ω_N relative to their counterparts in HMQC spectra, where Ω_N is given by

$$\Omega_N = k_a\left\{\frac{\xi_N}{(1+\rho)^2+\xi_N{}^2} - \frac{1}{2}\left[\frac{\xi_N+\xi_H}{(1+\rho)^2+(\xi_N+\xi_H)^2} + \frac{\xi_N-\xi_H}{(1+\rho)^2+(\xi_N-\xi_H)^2}\right]\right\} \quad (5)$$

with $\Omega_N/2\pi$ in Hz, $\xi_N = \Delta\omega_N/k_b$, and $\xi_H = \Delta\omega_H/k_b$. The presence of shift Ω is a consequence of the fact that exchange averaging in the single- and multiple-quantum manifolds is different. Indeed, exchange processes may be classified differently (slow-to-fast time scale) depending on whether they are detected via single-quantum coherences (characteristic exchange parameter $\Delta\omega_N/k_{ex}$) or multiple-quantum coherences (($\Delta\omega_N \pm \Delta\omega_H$)/$k_{ex}$). Since exchange averaging is nonlinear, the mean of the double- and zero-quantum frequencies (HMQC) does not coincide with the single-quantum frequency (HSQC), giving rise to the small shift Ω.

Considering Ω_N in eq 5 as a function of ξ_H, it can be shown that Ω_N has the same sign as ξ_N so long as $|\xi_N| < \sqrt{3}(1+\rho)$. In practice, this condition is fulfilled for intermediate-to-fast time scale chemical exchange. Assuming reasonable values of ΔR ($\sim$10 s^{-1}) and exchange in the microsecond-to-millisecond range ($k_{ex} \sim 1000$ s^{-1}, for example), ρ can be safely neglected, $|\rho| \ll 1$, and the above condition can be reformulated as

$$|\Delta\omega_N| < \sqrt{3}k_b \quad (6)$$

When this condition is met, the HSQC peak is positioned closer to the resonance of the invisible minor species than the corresponding HMQC peak (see Figure 1), and hence *analysis of these two spectra can provide the sign of $\Delta\omega_N$*.

Starting from eq 5 it can be shown that for a given value of ξ_N the maximum magnitude of the shift Ω_N occurs when $\xi_H = \pm\{[(\xi_N^2+1)^{1/2}+1]^2-1\}^{1/2}$. For very large ξ_H values the exchange-induced shift in HMQC spectra disappears and Ω_N derives only from the shift in HSQC spectra, $\Omega_N = k_a\xi_N/(1+\xi_N^2)$. Conversely, for vanishingly small ξ_H the exchange-induced shifts in HSQC and HMQC spectra are equal so that $\Omega_N = 0$. It is worth noting that Ω_N is essentially independent of differential relaxation ΔR (with the exception of the case where spins in state b are strongly relaxed by a paramagnetic center resulting in ΔR comparable to k_b). Further details about the functional dependence of Ω_N, eq 5, are given in the next section where exchange-induced shifts are investigated for the cavity mutant of the 162-residue protein L99A.

Application to the L99A Mutant of T4 Lysozyme

The L99A cavity mutant of bacteriophage T4 lysozyme has been extensively studied by a variety of techniques.[16−18,23,24] In particular, comprehensive studies of microsecond-to-millisecond time scale dynamics have been recently undertaken in our group[13,14,19,20] using new relaxation dispersion experiments based on the Carr−Purcell−Meiboom−Gill pulse sequence. Relaxation dispersion data for amide ^{15}N and methyl ^{13}C spins were found to be consistent with a single two-site exchange process with $k_{ex} = 1450$ s^{-1} and $p_b = 3.4\%$ at 25 °C. Exchanging sites were mapped onto the protein structure using $|\Delta\omega_N|$ and $|\Delta\omega_C|$ values determined for individual residues (119 and 72 residues, respectively). The exchange process has been localized to residues in the C-terminal domain of the protein and is very likely responsible for the entry (release) of small hydrophobic molecules into (from) the cavity. However, the mechanistic details of this process are largely unknown since the structure of the minor species has not been determined. To advance our understanding of this system, it is useful to examine spectra of the minor species that cannot be recorded directly because of the low population p_b and the exchange broadening that is present, but that can be reconstructed on the basis of relaxation dispersion data. Specifically, the resonance frequencies in question can be calculated as $\omega_b = \omega_a + \Delta\omega$, where the absolute value $|\Delta\omega|$ is known from relaxation dispersion experiments and ω_a is essentially the frequency of the single dominant peak appearing in the spectrum (in principle, a very small correction δ^{ex} can be included when calculating ω_a). The

(23) Eriksson, A. E.; Baase, W. A.; Matthews, B. W. *J. Mol. Biol.* **1993**, *229*, 747−769.
(24) Wray, J. W.; Baase, W. A.; Lindstrom, J. D.; Weaver, L. H.; Poteete, A. R.; Matthews, B. W. *J. Mol. Biol.* **1999**, *292*, 1111−1120.

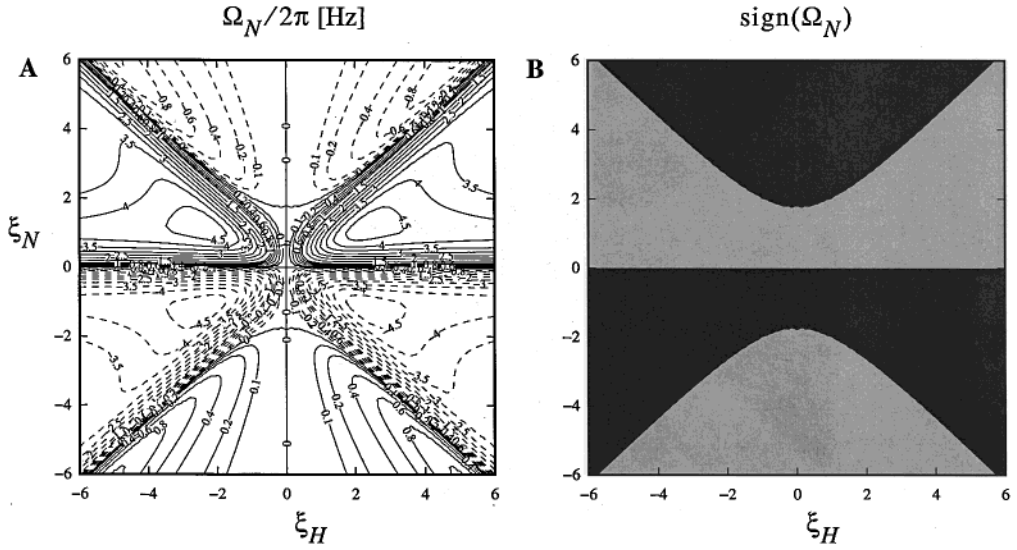

Figure 2. Shift Ω_N calculated according to eq 5 as a function of $\xi_H = \Delta\omega_H/k_b$ and $\xi_N = \Delta\omega_N/k_b$ assuming $k_{ex} = 1450\ s^{-1}$ and $p_b = 3.4\%$ as determined for chemical exchange in L99A at 25 °C.[19] The sign of Ω_N is color coded in panel B (dark shading corresponds to negative Ω_N). Note that Ω_N is a symmetric function of ξ_H, eq 5, and therefore the efficacy of our approach is independent of the sign of $\Delta\omega_H$.

only key element missing is the sign of $\Delta\omega$, which cannot be obtained from the relaxation dispersion data. With this in mind, we set out to determine the signs of $\Delta\omega_N$ using a combination of simple HSQC and HMQC spectra (we use the abbreviation H(S/M)QC in referring to this approach).

We begin by investigating how the shift Ω_N varies with ξ_H and ξ_N. The magnitude of Ω_N expected in L99A can be computed based on eq 5 as a function of ξ_H and ξ_N using fixed values of k_{ex} and p_b derived from relaxation dispersion analyses,[19] Figure 2, panel A. The sign of Ω_N is plotted in panel B, with light and dark shading corresponding to positive and negative values, respectively. As discussed above, the sign of Ω_N is defined unambiguously in the range $-\sqrt{3} < \xi_N < \sqrt{3}$, where the signs of Ω_N and ξ_N are the same; see panel B. In fact, the relaxation dispersion data indicate that for L99A at 800 MHz proton frequency ξ_N values for all but one residue fall within this range. For the single exception, Gly 110, $|\Delta\tilde{\omega}_N| = 5.33$ ppm, corresponding to $|\xi_N| = 1.92$, just above the threshold of $\sqrt{3}$.

Close inspection of Figure 2A reveals that in practice the range defined by eq 6 can be significantly extended. Consider, for example, a cross section through the surface in Figure 2A at $\xi_N = 2.5$. As can be seen from the plot, the highest positive value of Ω_N along this cross section is 4 Hz, while the lowest negative value is only -0.2 Hz. Since small shifts, such as -0.2 Hz, are ignored in the analysis because they cannot be measured with sufficient accuracy (see below), values of Ω_N above a certain threshold, as discussed below, unambiguously establish the sign of $\Delta\omega_N$.

In the case of L99A, only shifts Ω_N in excess of ~0.3 Hz were used to determine the sign of $\Delta\omega_N$. Hence, the application of the method is confined to the region of the map in Figure 2A where $|\xi_N| > \sim 0.04$ and $|\xi_H|$ is comparable to or greater than $|\xi_N|$. The first condition does not represent a significant limitation since very small chemical shift offsets ($|\xi_N| = 0.04$ corresponds to $|\Delta\tilde{\omega}_N|$ of 0.1 ppm at 800 MHz) cannot be quantified by relaxation dispersion methods in any case. The second condition is somewhat more restrictive. For example,

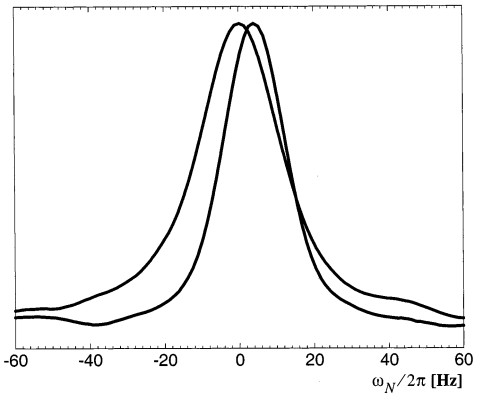

Figure 3. Spectral F1(^{15}N) traces through the cross-peak derived from residue Gly 113 of L99A in ^{1}H$-^{15}$N HSQC (sharp line shifted to the right) and HMQC (broad line centered at zero) spectra. The intensities are rescaled such that the heights of the two lines are equal, allowing for better visualization of the shift Ω_N. The spectra were recorded at 800 MHz, 25 °C, in 3 (HSQC) and 6 (HMQC) h. Regions of HSQC and HMQC correlation maps containing the peak from Gly 113 are shown in Figure S1. For the sake of comparison, this figure (S1) also includes the Gly 51 correlation that does not show any evidence of exchange.

for a typical value of $|\Delta\tilde{\omega}_N|$ of 2 ppm, $|\Delta\tilde{\omega}_H|$ must be at least 0.1 ppm. Our results (see below) indicate that as a rule $|\Delta\omega_H|$ is sufficiently large in the residues involved in chemical exchange to give rise to measurable Ω_N shifts.

To quantitate Ω_N values (4.3 Hz or less for L99A), we used a slightly modified version of the conventional HMQC sequence[25,26] intended to eliminate the deleterious effects of $^3J_{HN,H\alpha}$ scalar couplings that are active in most HMQC schemes (see Materials and Methods for the details of the pulse sequence). Figure 3 shows a pair of traces through the cross-peak from Gly 113 extracted from HSQC and HMQC spectra recorded on a 1 mM sample of uniformly ^{15}N,^{13}C-labeled L99A[14] at 800 MHz proton frequency. The position of the peak in the HSQC correlation map (more narrow line in the plot) is

(25) Müller, L. *J. Am. Chem. Soc.* **1979**, *101*, 4481−4484.
(26) Bax, A.; Ikura, M.; Kay, L. E.; Torchia, D. A.; Tschudin, R. *J. Magn. Reson.* **1990**, *86*, 304−318.

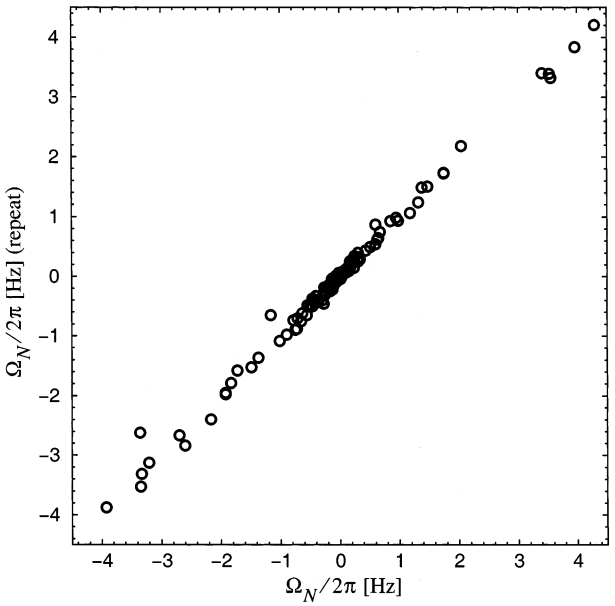

Figure 4. Exchange-induced shifts Ω_N (Hz) obtained from a pair of repeat HSQC−HMQC measurements of L99A at 25 °C. The positions of the peaks in the spectra have been initially extracted in ppm ($\tilde{\omega}_N$) and subsequently converted to Hz ($\tilde{\omega}_N/2\pi$) according to $\omega_N = \gamma_N B_0 \tilde{\omega}_N$, where γ_N is the negative gyromagnetic ratio of nitrogen.[22] Positive Ω_N values in Hz correspond, therefore, to the situation where the resonance of the invisible minor species is located upfield of the observable peak (see Figure 1 where Ω_N is positive).

clearly shifted relative to its position in the HMQC. The magnitude of the shift is 4.3 Hz, the largest of all shifts observed in L99A at 25 °C.

Figure 4 demonstrates a very good correlation between the values of Ω_N determined from two repeat H(S/M)QC measurements. The data sets are comprised of 124 experimentally measured backbone amide shifts, out of 158 potentially available in L99A, plus three tryptophan side chain shifts. Surprisingly accurate shift values can be obtained even for peaks with partial spectral overlap (at ca. 20% of their height), provided that each group of partially overlapped peaks is treated as a cluster during data fitting. Using the nonlinear fitting routine nlinLS,[27] we have been able to quantitate Ω_N for all but a few strongly overlapped peaks. The root-mean-square deviation (rmsd) between the pair of repeat measurements presented in Figure 4 is 0.11 Hz. For the 10 residues with the smallest shifts (i.e., lowest mean values of $|\Omega_N|$), the rmsd is only 0.04 Hz, while for the 10 residues with the largest shifts, including the single worst outlier in the correlation, it is 0.26 Hz. The difference in the two rmsd values can be understood by noting that the largest shifts are associated with broad, low-intensity peaks affected by chemical exchange. For these peaks measurement of $|\Omega_N|$ is, in relative terms, more susceptible to noise. The results shown in Figure 4 have been obtained from 6-h HMQC and 3-h HSQC experiments. Given the level of precision achieved in these measurements and the fact that the sensitivity of the HMQC experiment at 800 MHz is approximately 20% higher than that of the HSQC,[26] we conclude that in practice satisfactory results can be obtained with a pair of 1.5-h experiments.

By means of additional verification, we recorded zero- and double-quantum spectra of L99A. The details of the pulse sequences are not described here since the schemes are similar to those developed by Kloiber and Konrat.[28] In this approach the shift Ω_N, eq 5, can be evaluated based on the positions of peaks in the single-, zero-, and double-quantum correlation maps. It is clear that from our perspective this method, termed H(S/Z/D)QC, is inferior to the H(S/M)QC approach since (i) only peaks that are sufficiently well-resolved in three distinct spectra can be included, (ii) the pattern of partial spectral overlaps is different in each of the three spectra which makes determination of the relative shifts less accurate, and (iii) either the double- or zero-quantum peak is broader than the corresponding HMQC correlation due to contributions from exchange and cross-correlated relaxation.[28,29] Hence, the H(S/Z/D)QC experiment has been used strictly for verification. A total of 88 residues for which Ω_N has been determined by H(S/M)QC and, independently, by H(S/Z/D)QC experiments were considered. For the 10 residues with the smallest Ω_N values the rmsd between the two data sets is 0.14 Hz, whereas for the 10 largest shifts the uncertainty increases to 0.65 Hz. Importantly, for all residues with appreciable shifts (43 residues where $|\Omega_N/2\pi| >$ 0.3 Hz), both methods predict the same sign of Ω_N. This result provides strong support for the H(S/M)QC methodology described above.

In Figure 5A the shifts measured with H(S/M)QC experiments recorded on L99A are plotted as a function of residue number. When mapped onto the structure of the protein, Ω_N data confirm recent findings of Mulder et al.[19] indicating that microsecond-to-millisecond time scale dynamics is mainly concentrated in the vicinity of the C-terminal cavity. Notably, the largest effect is observed in helices E and F and the interceding loop which have been identified as the elements proximal to the site of entry of small hydrophobic ligands. In contrast, no shifts are observed in helix B and the adjacent structural elements which are farthest removed from the cavity (residues 33−64, average shift 0.08 ± 0.10 Hz).

As described above, eq 4, an alternative strategy for determination of the sign of $\Delta\omega_N$ involves comparison of a pair of HSQC spectra recorded at different magnetic field strengths (H(S/S)QC, see Materials and Methods for experimental details). To test this approach, two 4-h spectra were recorded on a 1 mM sample of L99A at spectrometer fields of 500 and 800 MHz, 25 °C. To be able to compare the chemical shifts of cross-peaks in the two HSQC spectra recorded on different spectrometers, the slight (and unavoidable) differences in experimental conditions, for example, differences in sample temperature, must be taken into account. To account for these differences, we have selected a group of peaks from residues 33−64 that are not affected by exchange, see Figure 5A, that can be used as an "internal reference" facilitating comparison of the two spectra. For these residues chemical shift data from the two fields were best fit according to the relation $\tilde{\omega}_N(500\ \text{MHz}) = 0.9996\tilde{\omega}_N(800\ \text{MHz}) + 0.2021$. The correction implied by this equation was subsequently applied to all of the data at 800 MHz prior to interpretation. Although H(S/S)QC shifts, $\tilde{\sigma}_N$, are intrinsically defined in units of ppm, eq 4, it is convenient to express them in Hz as well. Since H(S/S)QC measurements are performed at two different fields, the choice of conversion factor is somewhat arbitrary. We have chosen the conversion factor

(27) Delaglio, F.; Grzesiek, S.; Vuister, G. W.; Zhu, G.; Pfeifer, J.; Bax, A. *J. Biomol. NMR* **1995**, *6*, 277−293.
(28) Kloiber, K.; Konrat, R. *J. Biomol. NMR* **2000**, *18*, 33−42.
(29) Pervushin, K. V.; Wider, G.; Riek, R.; Wüthrich, K. *Proc. Natl. Acad. Sci. U.S.A.* **1999**, *96*, 9607−9612.

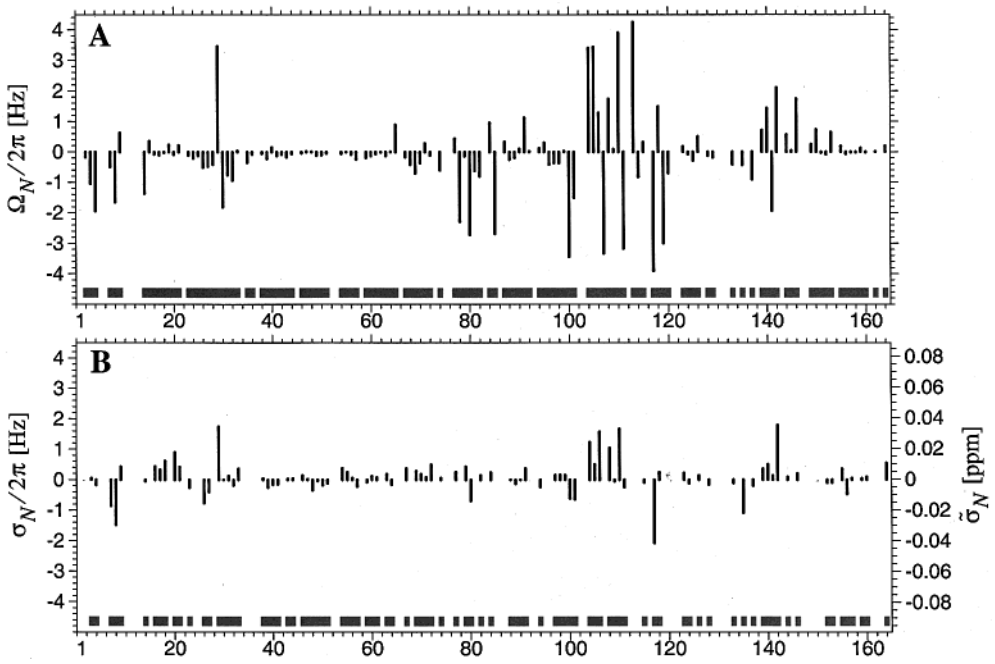

Figure 5. Exchange-induced shifts Ω_N (A) and σ_N (B) as a function of residue number in L99A at 25 °C. The shaded bars at the bottom part of the plots mark the residues for which data are available. The data in panel (B) have been originally obtained in ppm according to eq 4, vertical scale on the right-hand side of the plot, and subsequently converted to Hz assuming that 1 ppm = −50.5 Hz, vertical scale to the left.

associated with the lower field (500 MHz in our case; 1 ppm = −50.5 Hz for ^{15}N), so that smaller σ_N shifts (in Hz) are reported, Figure 5B, reflecting the fact that the errors are determined to a large extent by the uncertainty in peak positions in the spectrum recorded at lower field.

Shifts obtained from the H(S/S)QC combination are smaller and less reliable than those measured from the H(S/M)QC pair of experiments; cf. Figure 5A and 5B. As described above, the quality of the data is effectively limited by the 500 MHz experiment, where both sensitivity and spectral resolution are worse than at 800 MHz (as a result, only 92 shifts have been determined instead of 124 measured with the H(S/M)QC experiments). Nevertheless, excellent agreement between the two methods is obtained: for the 20 residues where both Ω_N and σ_N exceed 0.3 Hz, the signs of these two shifts coincide in all cases.

The magnitude of the Ω_N and σ_N shifts obtained in the present study can be verified on the basis of values extracted from fits of relaxation dispersion data recorded on L99A. In what follows we have made use of the exchange parameters obtained by Mulder et al.[19] in a comprehensive analysis of amide ^{15}N and methyl ^{13}C dispersion data: k_{ex} = 1450 s^{-1}, p_b = 3.4% at 25 °C. ^{15}N relaxation dispersion profiles recorded by Mulder et al. (data for 119 residues at 500 and 800 MHz) were fitted with the Carver−Richards equation[30,31] using fixed values for k_{ex} and p_b indicated above with $|\Delta\omega_N|$ optimized for each individual residue. It is not possible to calculate the magnitude of the expected H(S/M)QC shift, $|\Omega_N^{calc}|$, from $|\Delta\omega_N|$ alone since the former also depends on $\Delta\omega_H$, which is unknown. It is possible, however, to calculate the maximum magnitude of the shift $|\Omega_N^{calc}|$(max) using eq 5 and the expression for ξ_H that maximizes Ω_N (see Theory section above). The results of these calculations are presented in Figure 6A. The wedge-shaped region in the middle of the plot corresponds to the admissible range of Ω_N values predicted on the basis of the relaxation dispersion data for individual residues. Clearly, the observed shifts fit nicely into this range. In the case of H(S/S)QC-derived shifts, $|\sigma_N^{exptl}|$ can be directly compared with $|\sigma_N^{calc}|$ calculated according to eq 4 using values for k_{ex}, p_b, and $|\Delta\omega_N|$ determined from the relaxation dispersion data as described above. The correlation observed in Figure 6B is quite good considering that (i) the measured shifts are small, (ii) fits of the dispersion data can be sensitive to experimental error in the first place, and (iii) the two-site exchange model at the core of these analyses likely involves some degree of oversimplification.

As described above, the results of H(S/M)QC, H(S/S)QC, and H(S/Z/D)QC experiments are fully consistent when each of the measured shifts (Ω_N, σ_N) exceeds 0.3 Hz. We therefore consider the sign of $\Delta\omega_N$ to be reliable only in cases where the magnitude of Ω_N exceeds this value. Using this criterion, sign information has been obtained for 59 residues (Ala 146, which is an outlier in Figure 6A, has not been included). Combining this information with the results of relaxation dispersion analyses has allowed us to compile a list of 52 $\Delta\omega_N$ values, complete with the sign (44 of these are greater than 0.5 ppm). Notably, we have been able to unequivocally establish the sign for 18 of 19 residues where the magnitude of $\Delta\tilde{\omega}_N$ determined by relaxation dispersion measurements exceeds 1.5 ppm (the only exception is Glu 11, for which H(S/M)QC data are not available due to spectral overlap). Nearly all of these residues give rise to large Ω_N shifts (16 values in excess of 1 Hz). The signs determined by H(S/M)QC spectra have been confirmed by H(S/S)QC data sets in 15 of these cases (data unavailable for three residues because of spectral overlap). Finally, large Ω_N and σ_N shifts were obtained for Arg 8 and Asn 140 for which relaxation dispersion data were not available due to overlaps in CPMG-based spectra. This latter observation suggests that H(S/M)QC

(30) Carver, J. P.; Richards, R. E. *J. Magn. Reson.* **1972**, *6*, 89−105.
(31) Millet, O.; Loria, J. P.; Kroenke, C. D.; Pons, M.; Palmer, A. G. *J. Am. Chem. Soc.* **2000**, *122*, 2867−2877.

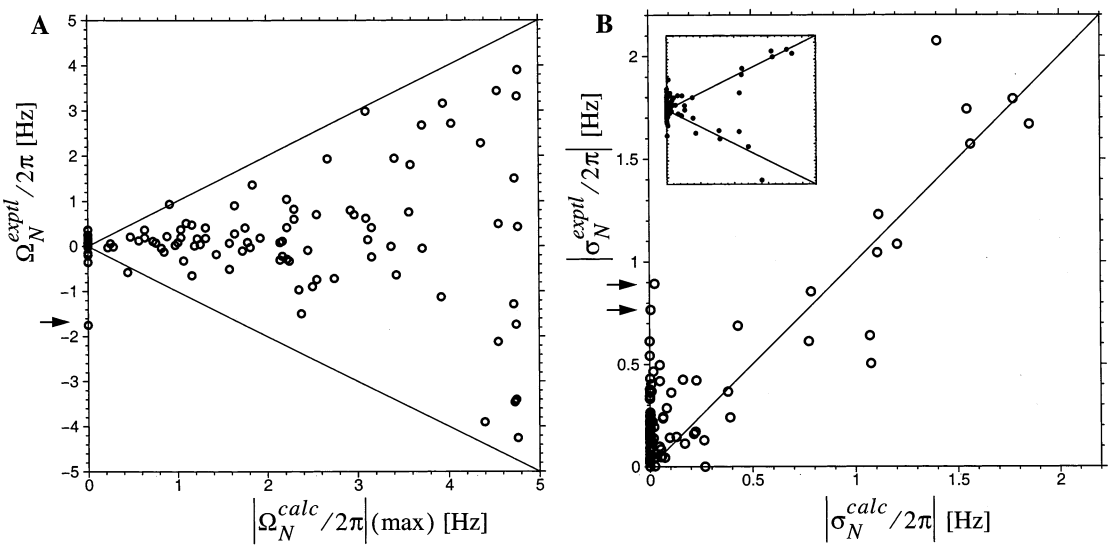

Figure 6. Comparison of experimentally determined exchange-induced shifts (Hz), Ω_N^{exptl} (A) and σ_N^{exptl} (B), with results of calculations based on relaxation dispersion data.[19] In panel A, the two lines dissecting the plot define the admissible Ω_N range, from $-\Omega_N^{calc}$(max) to Ω_N^{calc}(max), derived from the analyses of the relaxation dispersion data (see text). The reason for the single outlier, Ala 146 (identified by the arrow in the plot), is not entirely clear as both relaxation dispersion and σ_N data point toward very small exchange effects at this site. Two prominent outliers in panel B, Asp 20 and Thr 26 (identified by the arrows), are likely caused by spectral noise or artifacts since both relaxation dispersion and Ω_N data detect little exchange effects at these sites. The inset shows the analogue of the plot in panel B which includes the sign of σ_N^{exptl}.

and H(S/S)QC experiments can also be used as a simple qualitative probe to identify exchanging residues.

Concluding Remarks

It has long been recognized that information about chemical exchange is contained in the evolution of multiple-quantum coherences in the indirectly detected dimensions of two-dimensional experiments.[32−34] Here we present an example of how the combination of simple HSQC and HMQC data sets can provide useful information complementary to that available from relaxation dispersion studies of exchanging systems. Specifically, by comparing peak positions in HSQC and HMQC correlation maps, we have been able to obtain the signs of $\Delta\omega_N$ for 59 residues in L99A. Such sign information is difficult to obtain from other experiments. When combined with values for $|\Delta\omega_N|$ derived from relaxation dispersion experiments, this information can be used to determine chemical shifts for the excited (minor) state of the protein.

Simulations indicate that the H(S/M)QC methodology is potentially useful for the study of proteins with characteristic exchange times between ca. 0.1 ms and ca. 2 ms (upper bound derives from eq 6) and for minor state populations starting from less than 1%. (Note that for large p_b it may be necessary to use complete expressions for the eigenvalues of the matrix in eq 2; when p_b is sufficiently large to allow direct observation of the minor species, the approach described in the present work is obviously unnecessary). H(S/S)QC experiments can potentially be employed for the study of systems where the exchange time is in the range of ca. 0.1−10 ms and the population of the minor state is in excess of ∼3%. It should be emphasized, however, that from a practical viewpoint the applicability of H(S/M)QC and H(S/S)QC experiments should be analyzed in each individual case taking into account the specific values of the exchange parameters, p_b and k_{ex}, and chemical shift offsets, $|\Delta\omega|$, as well as other factors such as magnetic field strengths and sample concentration. The most important consideration in such analyses is that the exchange line broadening does not preclude accurate determination of chemical shifts. For example, for the exchanging residues in L99A T4 lysozyme, line widths are often dominated by R^{ex} contributions which exceed intrinsic relaxation rates, R_a and R_b. As a result, increases in R_a and R_b have only limited impact on the observed line widths. This suggests that, in principle, proteins twice the size of L99A can be successfully studied using the H(S/M)QC approach.

The approach that we have described here is by no means limited to backbone ^{15}N spins and can be readily extended to other nuclei. For example, in the case of the amide proton shift, Ω_H can be defined simply by interchanging the labels *N* and *H* in eq 5. Experimental results for Ω_H (not shown) show trends similar to those illustrated in Figure 5. Unfortunately, we have not been able to measure Ω_H at an acceptable level of precision in experiments performed to date (precision of ca. 1 Hz). The difficulties in studying slow dynamics using ^{1}H probes are well-known, and special measures, such as use of perdeuterated proteins, are required to overcome these problems.[35] Perhaps the most useful future extensions of our method will involve ^{13}C probes.

It has been previously suggested[19,36] that millisecond-time-scale dynamics in L99A involve "mobile structural defects" or local unfolding events that provide a route for ligand entry into the cavity. We used the results of the present work and a previous relaxation dispersion study[19] to calculate ^{15}N backbone chemical shifts for 52 residues within the spectroscopically invisible minor species of L99A. These shifts were subsequently compared with random-coil values computed for L99A using a

(32) Gamliel, D.; Luz, Z.; Vega, S. *J. Chem. Phys.* **1988**, *88*, 25−42.
(33) Rance, M. *J. Am. Chem. Soc.* **1988**, *110*, 1973−1974.
(34) Szymanski, S. *J. Magn. Reson. A* **1993**, *115*, 254−256.
(35) Ishima, R.; Wingfield, P. T.; Stahl, S. J.; Kaufman, J. D.; Torchia, D. A. *J. Am. Chem. Soc.* **1998**, *120*, 10534−10542.
(36) Eriksson, A. E.; Baase, W. A.; Wozniak, J. A.; Matthews, B. W. *Nature* **1992**, *355*, 371−373.

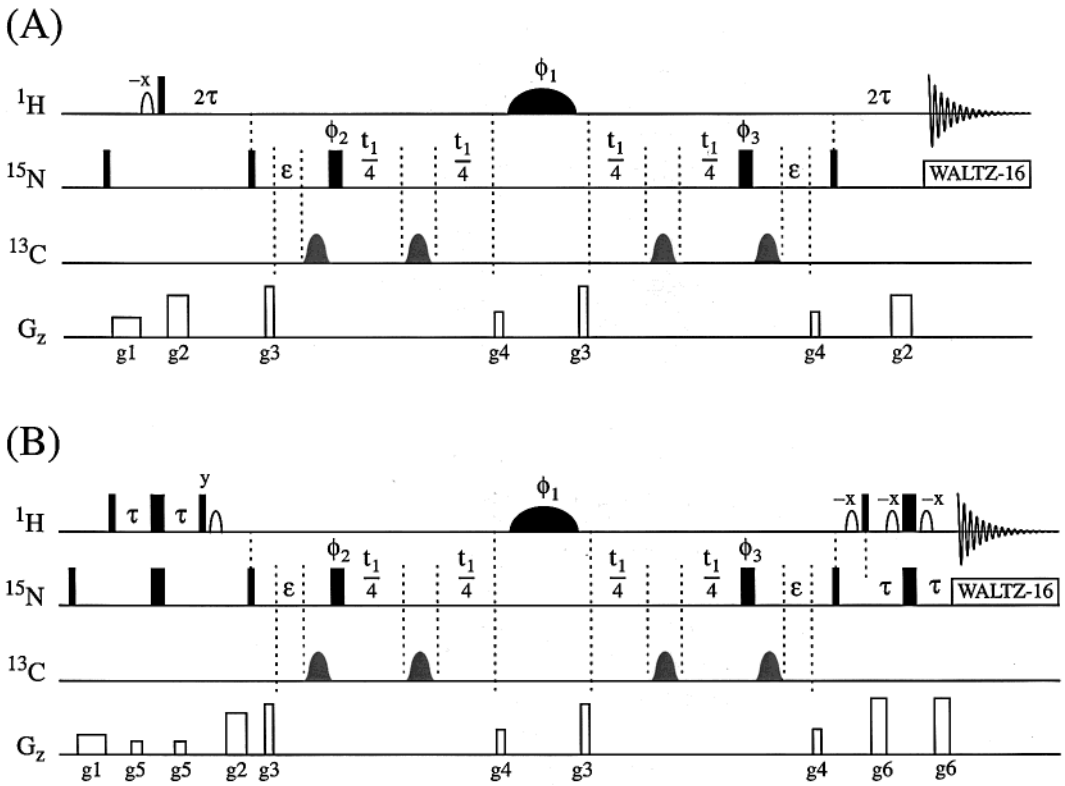

Figure 7. HMQC (A) and HSQC (B) pulse sequences used for measurement of Ω_N. All narrow (wide) rectangular pulses are applied with a flip angle of 90° (180°) along the *x*-axis unless indicated otherwise. The rectangular ^{1}H (^{15}N) pulses are centered at 4.77 ppm (119 ppm). Proton shaped pulses indicated in outline (i.e., not filled) are 90° water-selective SEDUCE-1 pulses[47] (1.5−2 ms duration). Filled proton shaped pulses (180°) have the RE-BURP profile[40] and are applied at 8.35 ppm with durations of 1.6 (2.5) ms and peak field strengths of 3.9 (2.5) kHz at 800 (500) MHz. Carbon 180° shaped pulses (0.4 ms duration) employ the WURST profile[43,44] and are centered at 117 ppm with a field strength of 11.4 kHz. ^{15}N WALTZ-16 decoupling[48] during acquisition employs a 1 kHz field. The delay ε is equal to half of the duration of the proton RE-BURP pulse and $\tau = 2.30$ ms. The phase cycle is $\phi_1 = \{x, y, -x, -y\}$, $\phi_2 = \{2x, 2y, 2(-x), 2(-y)\}$, $\phi_3 = \{4x, 4y, 4(-x), 4(-y)\}$, and rec = $\{x, 2(-x), x, -x, 2x, -x\}$ for the HMQC experiment while for the HSQC experiment rec = $\{2x, 4(-x), 2x\}$. Quadrature detection in F1 is accomplished by States-TPPI of the 90° ^{15}N pulse immediately preceding the evolution period.[49] The durations and strengths of the gradients are g1 = (2.0 ms, 8 G/cm), g2 = (1.0 ms, 15 G/cm), g3 = (0.05 ms, 20 G/cm), and g4 = (0.05 ms, 10 G/cm), and for the gradients used only in the HSQC sequence g5 = (0.05 ms, 4 G/cm) and g6 = (0.125 ms, 25 G/cm). The spectra at 800 MHz were recorded with acquisition times of 78 (t_1) and 128 (t_2) ms.

recently developed CSI module[37] interfaced with the NMRView program.[38]

If the local unfolding hypothesis is correct, one might expect that the chemical shifts of the minor species, $\tilde{\omega}_N^b$, would be closer to random-coil values than the shifts of the dominant conformer, $\tilde{\omega}_N^a$. In particular, this trend can be expected in the vicinity of the F-helix which was previously identified by crystallographic and NMR studies as the most mobile element of the C-domain scaffold.[39,18,19] Indeed, we have found that $\tilde{\omega}_N^b$ values are significantly closer to random-coil values for residues 105−107, 111, 113−114, and 118. However, the opposite is obtained for residues 108 and 110. It is likely that the local unfolding at this site does not lead to the formation of a true random coil since some of the dihedral angles most probably remain partially constrained due to interactions with other elements of the tertiary structure. Furthermore, $\tilde{\omega}_N^b$ values for other regions involved in millisecond-time-scale motion, such as helix A, on average are not closer to those expected for a random coil. The results suggest, therefore, that the unfolding event is localized around helix F. Perhaps this short strained segment may undergo a dynamic transformation which leads to a subtle rearrangement of other structural elements comprising the C-terminal domain. Large displacements of backbone atoms in this region (as much as 2 Å) have been previously observed in X-ray crystallographic studies of ligand binding to L99A.[39] It is likely that application of the methodology presented here to studies involving ^{13}C NMR, where chemical shifts can be very sensitive to secondary structure, will shed further light on the structural features of the excited state of this protein.

Materials and Methods

The pulse sequences used to record H(S/M)QC spectra are shown in Figure 7. In the HMQC scheme, Figure 7A, a selective RE-BURP pulse[40] is used to refocus proton chemical shift evolution during t_1. This pulse acts on HN protons without perturbing Hα magnetization so that evolution due to the three-bond scalar coupling, $^3J_{HN,H\alpha}$, is refocused immediately prior to acquisition.[41,42] This ensures that pure-absorptive line shapes are recorded in F1 and F2. In the case of applications to ^{13}C-labeled samples, evolution due to carbon−nitrogen scalar coupling during t_1 is suppressed by application of broad-band WURST inversion pulses.[43,44] Two compensatory delays of duration ε

(37) Schwarzinger, S.; Kroon, G. J. A.; Foss, T. R.; Chung, J.; Wright, P. E.; Dyson, J. H. *J. Am. Chem. Soc.* **2001**, *123*, 2970−2978.
(38) Johnson, B. A.; Blevins, R. A. *J. Chem. Phys.* **1994**, *29*, 1012−1014.
(39) Morton, A.; Matthews, B. W. *Biochemistry* **1995**, *34*, 8576−8588.
(40) Geen, H.; Freeman, R. *J. Magn. Reson.* **1991**, *93*, 93−141.
(41) Ponstingl, H.; Otting, G. *J. Biomol. NMR* **1998**, *12*, 319−324.
(42) Permi, P.; Kilpeläinen, I.; Annila, A.; Heikkinen, S. *J. Biomol. NMR* **2000**, *16*, 29−37.
(43) Böhlen, J. M.; Rey, M.; Bodenhausen, G. *J. Magn. Reson.* **1989**, *84*, 191−197.
(44) Kupce, E.; Freeman, R. *J. Magn. Reson., Ser. A* **1995**, *115*, 273−276.

are inserted into the HMQC sequence to refocus ^{15}N chemical shift evolution during the proton RE-BURP pulse. To facilitate comparison between HMQC and HSQC experiments, the HSQC pulse scheme has also been modified, Figure 7B, so that the evolution periods in both sequences are identical.

A standard HSQC sequence with WATERGATE water suppression[45] and a water flipback scheme[46] has been employed to record the pair of H(S/S)QC spectra (500 and 800 MHz). A carbon WURST pulse[43,44] was inserted in the middle of the t_1 evolution period to refocus evolution due to nitrogen−carbon couplings.

A 1 mM sample of uniformly ^{15}N,^{13}C-labeled T4 lysozyme (with the point mutations C54T/C97A/L99A), 50 mM sodium phosphate, 25 mM sodium chloride, pH = 5.5, was employed in all experiments. The experiments have been recorded on Varian Inova 800 and 500 MHz spectrometers at 25 °C (rotational correlation time of L99A is 10.8 ns[18]). To minimize temperature differences between spectra recorded on the different instruments, temperature calibrations were performed using methanol as a reference. In addition, a thermocouple placed inside a reference NMR tube loaded with buffer was also used for calibration. The ^{15}N backbone relaxation dispersion data kindly provided by F. Mulder and A. Mittermaier was recorded on an ^{15}N-labeled sample prepared with the same buffer as described above. The set of residues investigated in the present work is very similar, but not identical, to the one selected in relaxation dispersion studies (ca. 95% similarity). Several residues were classified as being overlapped in one study but not in the other due to slight differences in sample conditions, different experimental schemes (the CPMG study is based on HSQC spectroscopy), and different (subjective) criteria for identifying spectral overlaps.

Both spectra in the H(S/M)QC experiment were comprised of 408 × 1634 real points, processed using squared sine bell apodization functions, and zero-filled to 2048 × 8192 real points. The spectra were processed using the nmrPipe/nmrDraw software package,[27] and the resonance frequencies of the individual peaks were determined using the nonlinear fitting routine nlinLS from the same suite of programs. H(S/S)QC spectra were comprised of 384 × 1024 (500 MHz) and 384 × 1636 (800 MHz) real points and processed in the same manner.

Acknowledgment. Stimulating discussions with D. M. Korzhnev, A. Mittermaier (University of Toronto), V. Y. Orekhov (Goteborg University), and F. A. A. Mulder (University of Lund) are gratefully acknowledged. This work was supported by a grant from the Canadian Institutes of Health Research (CIHR). N.R.S. acknowledges support from CIHR in the form of a Centennial Fellowship. L.E.K. holds a Canada Research Chair in Biochemistry.

Supporting Information Available: List of 52 $\Delta\omega_N$ values (including sign) for L99A; figure showing selected regions of HSQC and HMQC correlation maps of L99A(PDF). This material is available free of charge via the Internet at http://pubs.acs.org.

JA0207089

(45) Piotto, M.; Saudek, V.; Sklenár, V. *J. Biomol. NMR* **1992**, *2*, 661−665.
(46) Grzesiek, S.; Bax, A. *J. Am. Chem. Soc.* **1993**, *115*, 12593−12594.
(47) McCoy, M.; Mueller, L. *J. Am. Chem. Soc.* **1992**, *114*, 2108−2110.
(48) Shaka, A. J.; Keeler, J.; Frenkiel, T.; Freeman, R. *J. Magn. Reson.* **1983**, *52*, 335−338.
(49) Marion, D.; Ikura, M.; Tschudin, R.; Bax, A. *J. Magn. Reson.* **1989**, *85*, 393−399.